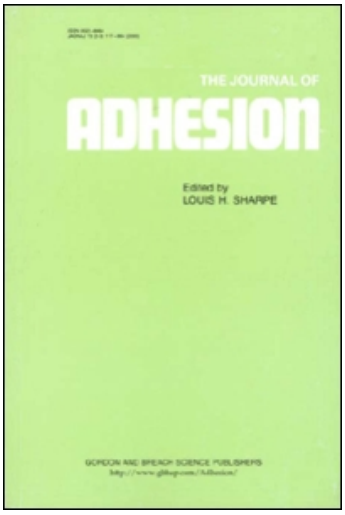

The Journal of Adhesion
Publication details, including instructions for authors and subscription information:
http://www.informaworld.com/smpp/title~content=t713453635

Relationship Between Viscoelastic and Peeling Properties of Model Adhesives. Part 2. The Interfacial Fracture Domains

C. Derail[a]; A. Allal[a]; G. Marin[a]; Ph. Tordjeman[b]
[a] Laboratoire de Physique des Matériaux Industriels, Université de Pau et des Pays de l'Adour, Pau, France [b] ElfAtochem, Groupement de Recherches de Lacq, Lacq, France

To cite this Article Derail, C. , Allal, A. , Marin, G. and Tordjeman, Ph.(1998) 'Relationship Between Viscoelastic and Peeling Properties of Model Adhesives. Part 2. The Interfacial Fracture Domains', The Journal of Adhesion, 68: 3, 203 — 228
To link to this Article: DOI: 10.1080/00218469808029255
URL: http://dx.doi.org/10.1080/00218469808029255

J. Adhesion, 1998, Vol. 68, pp. 203–228
Reprints available directly from the publisher
Photocopying permitted by license only

Relationship Between Viscoelastic and Peeling Properties of Model Adhesives. Part 2. The Interfacial Fracture Domains

C. DERAIL[a], A. ALLAL[a], G. MARIN[a,*] and PH. TORDJEMAN[b]

[a] *Laboratoire de Physique des Matériaux Industriels, Université de Pau et des Pays de l'Adour, 64000 Pau, France;*
[b] *ElfAtochem, Groupement de Recherches de Lacq, 64170 Lacq, France*

(Received 11 March 1997; In final form 26 January 1998)

The viscoelastic and peeling properties of polybutadiene/tackifying resin compatible blends have been studied in detail. Viscoelastic properties have been described through the variations of the complex shear modulus, $G^*(\omega)$, as a function of frequency, ω, and peeling properties through the variations of peeling force (F) as a function of peeling rate (V).

The first paper of this series presented the cohesive fracture domain and the present paper explores the interfacial fracture domain: (i) rubbery interfacial (interfacial 1); (ii) stick-slip; (iii) glassy interfacial (interfacial 2). After a general survey of the properties in the three domains we present a quantitative relationship between the peeling and linear viscoelastic properties as a function of the adhesive formulation, discussing the use of time-temperature equivalence for adhesive properties. The third part of the paper presents the trumpet model of de Gennes describing the crack shape and propagation: starting from a mechanical analysis of the peeling test, it is shown how one may calculate the variations of the peeling force as a function of peeling rate in the various interfacial fracture domains: this model defines a single interfacial fracture criterion which coexists with the cohesive fracture criterion defined earlier, whatever the fracture location.

We present as a conclusion a critical discussion of the relevance and physical meaning of such a criterion and present a new outlook for the modeling and improvement of adhesive formulations.

Keywords: Hot-melt adhesives; pressure-sensitive adhesives; adhesive joints; peeling; viscoelasticity; rheology; cohesive failure; interfacial failure; stick-slip; adhesive formulation; master curve; peeling and rheological parameters; trumpet model of de Gennes; complex shear modulus; time-temperature equivalence; blends of monodisperse polybutadiene with tackifying resin; mechanical spectroscopy

*Corresponding author.

1. INTRODUCTION

The ability to forecast the rheological and peeling properties of adhesives is an important issue for the improvement of adhesive formulation which is, for the most part, a mainly empirical process at the present time. As the qualitative link between viscoelastic and adhesive properties is now well established [1 – 4], we propose in this series of articles to present a quantitative relationship between the viscoelastic properties and adhesive properties (characterized by peeling measurements) of model hot-melt formulations. The first paper dealt with the first part of the peeling curves, *i.e.*, cohesive fracture. A quantitative relationship between the peeling curve and the viscoelastic properties in the terminal (low frequency) region of relaxation was established. A peeling master curve (peeling force as a function of reduced peeling rate, $V\tau_0$) could be constructed, τ_0 being the characteristic relaxation time of the terminal region of relaxation measured by mechanical spectroscopy experiments.

In the present paper, we will be dealing with the two regions of stable interfacial fracture as well as the unstable fracture domain known as "stick-slip". We will try to derive qualitative relations between viscoelastic and adhesive properties in these higher peeling rate domains. We will show that the temperature shift factors determined in rheology and peeling experiments are still the same, so time-temperature superposition [5] seems to apply whatever the fracture mode. Then we will propose a model of the interfacial fracture domain integrating the detailed mechanical analysis of the peeling test proposed in Refs. [1] and [3]. The fracture criterion selected in the interfacial fracture domain(s) is related to the "trumpet" model of fracture proposed by de Gennes [6].

This approach, although tentative and incomplete in some aspects, apprehends reasonably the fundamental features of adherence of viscoelastic materials. Besides, it gives a quantitative tool for the improvement of adhesive formulation.

2. EXPERIMENTAL

2.1. Samples

The model formulations are made of blends of a monodisperse polybutadiene with a tackifying resin. The basic polymers are quasi-

monodisperse anionic polybutadiene samples of the same microstructure [3] which have been synthetized by the Michelin company (France); the tackifying resin is a terpene-phenolic resin (Dertophene T) from the D.R.T company (France). This resin is an unentangled oligomer which has a double effect: a "topological" effect which swells the entanglement network of the polymer and a thermodynamic effect which increases the glass transition temperature of the formulation (antiplastifying effect) [4]. Sample preparation has been described in our previous paper [1]. The compositions of the various formulations and their glass transitions temperatures are reported in Table I. The molecular weights of samples PB1 and PB2 are respectively 150000 and 65000 g/mol.

2.2. Rheology

Rheological characterization of our adhesives was done by measuring the complex shear modulus, G^*, as a function of frequency, ω, at various temperatures. These mechanical spectroscopy experiments were performed in the frequency range $10^{-2}-500\,\mathrm{rd\,s^{-1}}$ using a Rheometrics RDA700 rotational rheometer in a parallel-plate geometry. The use of the time-temperature superposition principle allows one to plot master curves which feature the main relaxation domains, from the terminal relaxation region (flow region) up to the glassy behavior (α-relaxation) at high frequencies. Sample characteristics and their rheological parameters are summerized in Table I. The rheological master curves corresponding to a very broad frequency range covering the relaxation domains ranging from the flow region (lowest frequencies) to the α (glass transition) are reported on Figures 1 to 3. The solid lines in Figure 2 have been calculated from a molecular model derived from the reptation theory which has been successfully applied to a large number of linear polymers [7, 3]. This model describes the relaxation of entangled polymers as a succession of four relaxation processes, each being governed by a characteristic relaxation time defined by the chain structure. This model may also be applied to concentrated solutions of polymers, which is the case for Hot-Melt and PSA formulations: in that case, the variations of the viscous and elastic (plateau modulus, limiting compliance) properties of the formulations may be predicted with a very good accuracy as a function of polymer volume fraction.

TABLE I Composition of the various formulations, their glass transitions (thermomechanical analysis) and main rheological parameters: zero-shear viscosity, average relaxation time, plateau modulus and limiting compliance

	20*PB*180	25*P*175	30*PB*170	35*PB*165	40*PB*160	45*PB*155	*PB*1	30*PB*270	*PB*2
ϕ(%)	20	25	30	35	40	45	100	30	100
η_0 (Pa · s)	$4.92\ 10^3$	$5.56\ 10^6$	$2.78\ 10^6$	$8.00\ 10^5$	$3.26\ 10^5$	$9.69\ 10^4$	$1.18\ 10^5$	$1.09\ 10^4$	$5.62\ 10^3$
τ_0(min)	$4.20\ 10^{-3}$	2.38	0.88	0.25	$5.8\ 10^{-2}$	$2\ 10^{-2}$	$2.4\ 10^{-3}$	$5.7\ 10^{-3}$	$2.21\ 10^{-4}$
G_N^0(Pa)	$3.00\ 10^4$	$6.40\ 10^4$	$8.46\ 10^4$	$1.30\ 10^5$	$2.00\ 10^5$	$2.50\ 10^5$	$1.20\ 10^6$	$8.46\ 10^4$	$1.20\ 10^6$
J_e^0(Pa^{-1})	$5.12\ 10^{-5}$	$2.57\ 10^{-5}$	$1.89\ 10^{-5}$	$1.80\ 10^{-5}$	$1.07\ 10^{-5}$	$9.21\ 10^{-6}$	$1.20\ 10^{-6}$	$3.16\ 10^{-5}$	$2.37\ 10^{-6}$
Tg(°C)	–	−1	−6	−17	−30	−41	−88	−6	−88

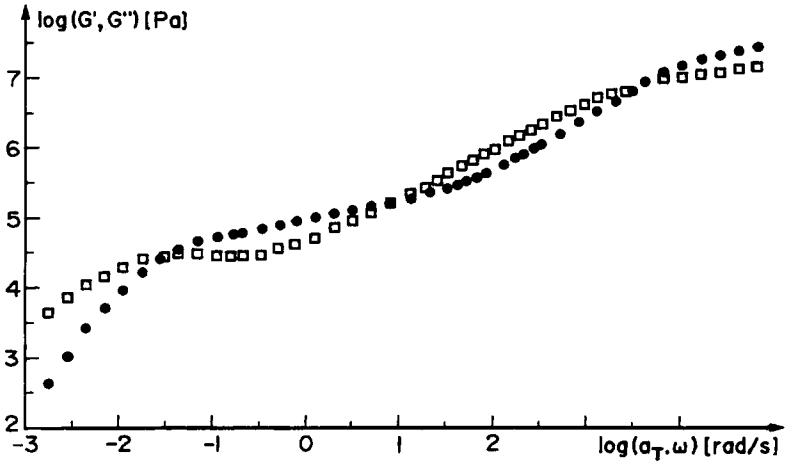

FIGURE 1 Master curve of mechanical spectroscopy for sample 30PB170: storage (●:G') and loss (□: G'') moduli as a function of frequency (reference temperature T_0 = 25°C).

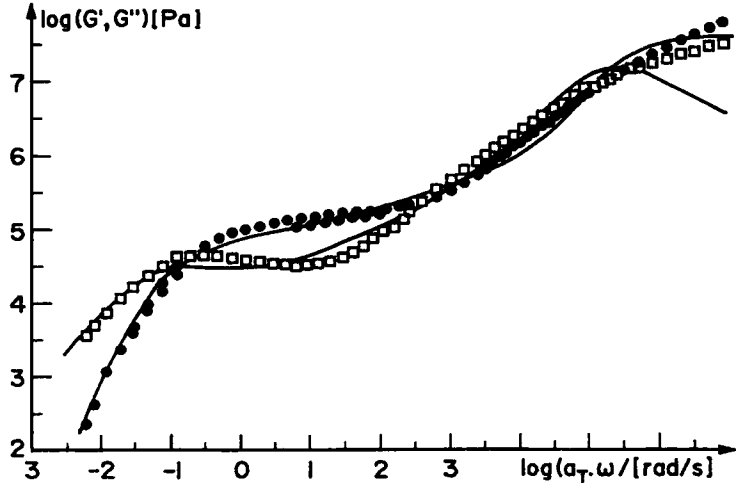

FIGURE 2 Master curve of mechanical spectroscopy for sample 35PB165: storage (●:G') and loss (□: G'') moduli as a function of frequency (reference temperature T_0 = 25°C). Solid lines have been calculated from a molecular dynamics model [7].

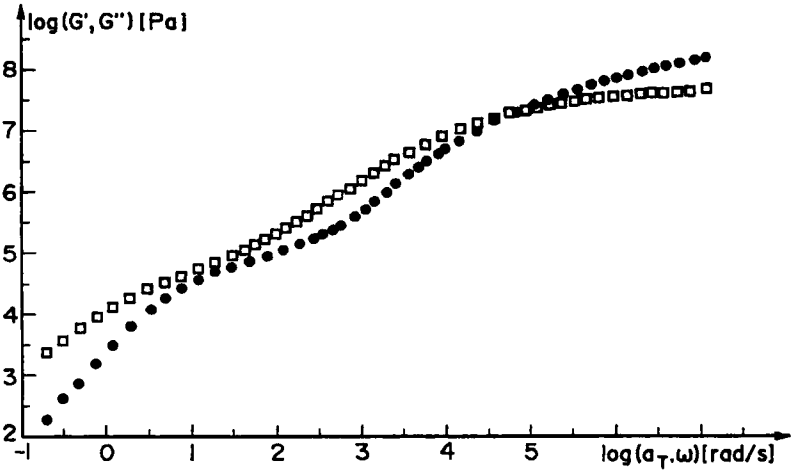

FIGURE 3 Master curve of mechanical spectroscopy for sample 30PB270: storage (●:G') and loss (□: G'') moduli as a function of frequency (reference temperature $T_0 = 25°C$).

2.3. Peeling

Peeling experiments were performed on an Adamel Lhomargy DY 30 tensile machine which was equiped with an environmental chamber. We have performed isothermal experiments, measuring the peeling force as a function of peeling rate at each temperature. The available peeling rate range was 1 to 1000 mm/min and temperature range −50 to 120°C, so we have been able to characterize all peeling modes for every formulation.

We have selected the ASTM D 3167-76 normalized peeling test, which is a "floating rollers" test, at constant peeling rate (see Ref. [3]). The peeling samples are sandwich-type probes made of three parts:

- a flexible aluminium substrate (thickness: 104 μm), which is often assumed to be non-extensible [1]. The only surface treatment of that substrate was a thorough cleaning with acetone.
- a rigid aluminium substrate (thickness: 2 mm). In order to control its surface quality, the rigid aluminium substrates was sanded in a controlled way.

- the adhesive itself was pressed between the aluminium substrates in several steps and at elevated temperature (80°C) in order to reach a standard gap of 130 μm.

Each probe was carefully prepared and the adhesive thickness was controlled using an electronic micrometer. The uncertainty in adhesive thickness may be estimated to be 10%.

The peeling curves (peeling force as a function of peeling rate) have been shown to be "rheological curves" in the sense that they obey time-temperature equivalence [5]. The master peeling curves are reported on Figures 4 to 6; the detailed procedure for the peeling tests has been detailed in Refs. [1] and [3]. The various fracture modes observed are recalled on Figure 4. The first part of the peeling curves, corresponding to the cohesive fracture mode, has been thoroughly described and studied in Ref. [1]; in the same paper, a predictive model of the rheological and peeling behavior had been presented for cohesive fracture. We will deal in the present paper with the other fracture modes which appear at higher peeling rates and correspond to a different fracture location and to the occurrence, in some cases, of fracture instability.

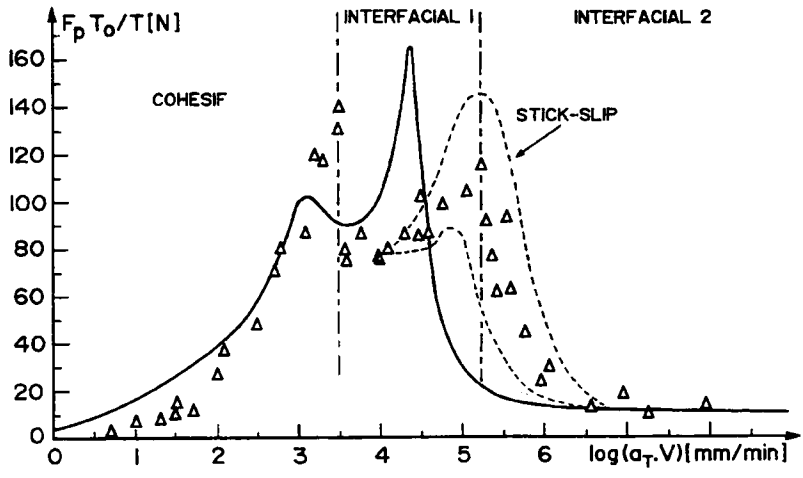

FIGURE 4 Peeling force as a function of reduced peeling rate ($a_T V$). Master curve at 25°C for samples 30PB170. The solid line has been calculated from our model (Ref. [1]).

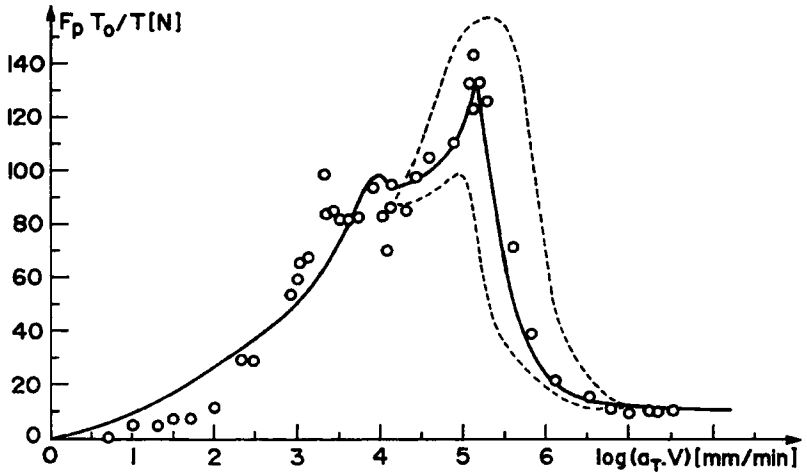

FIGURE 5 Peeling force as a function of reduced peeling rate ($a_T V$). Master curve at 25°C for samples 35PB165. The solid line has been calculated from our model (Ref. [1]).

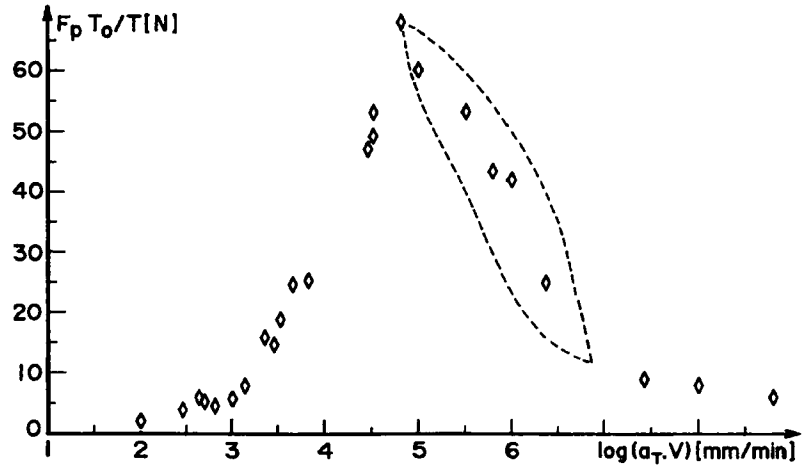

FIGURE 6 Peeling force as a function of reduced peeling rate ($a_T V$). Master curve at 25°C for samples 30PB270.

3. QUALITATIVE RELATIONS BETWEEN VISCOELASTIC AND PEELING PROPERTIES

3.1. "Type 1" Interfacial Fracture Domain

The interfacial 1 (or I_1) domain follows the cohesive fracture domain and corresponds to a fracture mode where the crack propagates between the adhesive and the rigid aluminium substrate [1].

One may observe that, at the same resin content, the viscoelastic behavior of blends formulated from PB1 and PB2 may be quite different. This effect of polymer molecular weight is exhibited on Figures 1 and 3: sample 30PB170 exhibits a well-marked elastic plateau at intermediate frequencies, whereas the elastic plateau seems non-existent for sample 30PB270 which is still, however, in the entangled domain (see Appendix). The viscoelastic behavior of that last sample is close to what is observed for commercial Hot-Melt adhesives [8]. In that case, the various viscoelastic relaxation domains are strongly coupled and it is more difficult to differentiate between them.

The peeling behavior exhibited on Figures 4 and 6 is also quite different. One may observe on Figure 4 that sample 30PB170 exhibits all four fracture domains already described (cohesive/interfacial 1/stick-slip/interfacial 2), whereas the interfacial 1 fracture domain has disappeared for sample 30PB270 in Figure 6: one shifts directly from cohesive fracture to a stick-slip behavior as the peeling rate increases. This type of behavior is also observed for most commercial Hot-Melts for which there is no type 1 interfacial fracture. One may observe also that the width of the interfacial 1 fracture domain diminishes with the width of the plateau region in the frequency (or time) scale. This had already been observed with our samples [3] and the data of Aubrey [9] on other formulations leads to the same conclusion. The addition of resin to the polymer diminishes the width of the elastic plateau region but also decreases the plateau modulus value [1, 8]; the gradual disappearing of the type 1 interfacial fracture is probably due to both effects. We may then conclude that the viscoelastic feature which is to relate to the type 1 interfacial fracture is a well-established plateau modulus ($G' > G''$): hence we will call this fracture domain the "rubbery fracture domain". A precise relation between the broadness

of the rubbery plateau domain and the I_1 fracture domain would necessitate, however, a comprehensive study using polymer samples covering a broad range of molecular weights, at same resin content. Changing the resin content changes the plateau modulus value and extent, but also changes the glass transition temperature, so all these combined effects do not lead to a simple relationship. A thorough study of the effect of polymer molecular weight would permit one to discriminate between these two effects (plateau modulus value/extent) [10].

One may notice also that a stick-slip behavior appears in the interfacial 1 domain for samples 30PB170 and 35PB165 at higher peeling rates. This is, to our knowledge, the first time such a behavior is described. The stick-slip behavior is different from the usual stick-slip observed in the interfacial 2 domain: the main differences are the fracture location and low amplitude of the force oscillations. This behavior has been observed for other formulations made from sample PB1 for which a minimum is observed in the $G''(\omega)$ curve; such a minimum is never observed for commercial formulations and more generally for polymers presenting a broad distribution of molecular weights. Hence, this peculiar behavior may be attributed to the fact that we are using model (*i.e.*, nearly monodisperse) polymers (Fig. 7).

3.2. "Interfacial 2" and "Stick-slip" Fracture Domains

In the interfacial 2 (or I_2) domain, fracture propagates between the flexible aluminium substrate and the adhesive [1, 3]. We have already demonstrated [1] that cohesive fracture was correlated with the viscoelastic properties in the terminal region of relaxation which corresponds to the longest relaxation times. The I_1 fracture behavior being linked to the viscoelastic properties in the plateau region, it is straightforward to relate the stick-slip instability to the viscoelastic transition region between the rubbery plateau (characterized by the plateau modulus) and the glassy behavior (characterized by the glassy modulus G_∞) (see Fig. 8). This transition is the mechanical analog of the glass transition, T_g, measured using thermal analysis (DSC or DTA). In our case, the glassy modulus, G_∞, has roughly the same value for all formulations, close to a value corresponding to the bulk polymer ($G_\infty \approx 3 \times 10^8$ Pa). The peeling force keeps approximately the

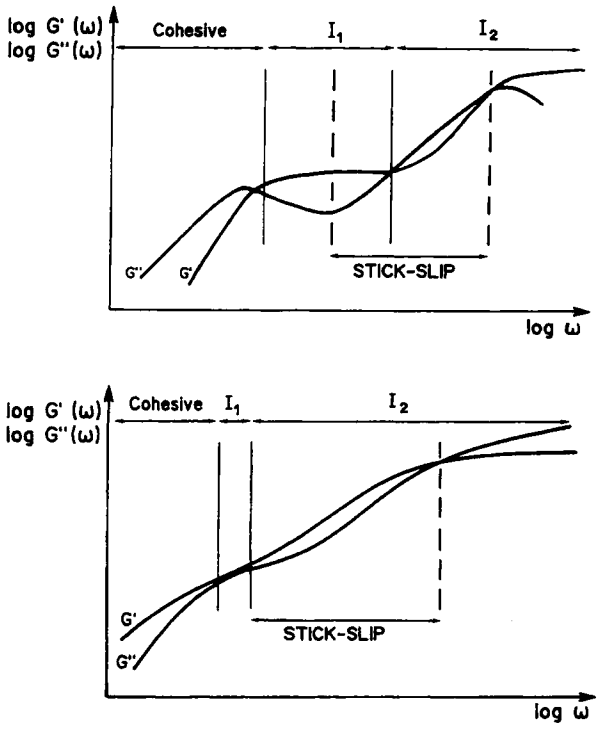

FIGURE 7 Stick-slip in the I_1 interfacial domain.

same relatively small value ($F \approx 10$ N) after the stick-slip domain whatever the formulation. We did not observe any of the inertia effects described by Maugis [11] on our testing machine.

In the stick-slip region, stripes perpendicular to the direction of fracture are observed on both the adhesive and the flexible substrate. Optical micrographs of the side of the aluminium foil showed evidence of plastic deformation: one may observe a large black band which proves, in addition to a remaining deformation after the experiment, that the substrate has experienced a plastic deformation. The stripes are also located on that same plastic deformation zone.

In the I_2 interfacial domain, the behavior is qualitatively equivalent to what happens in the rubbery interfacial (I_1) domain, with the difference that fracture occurs between the adhesive and the flexible

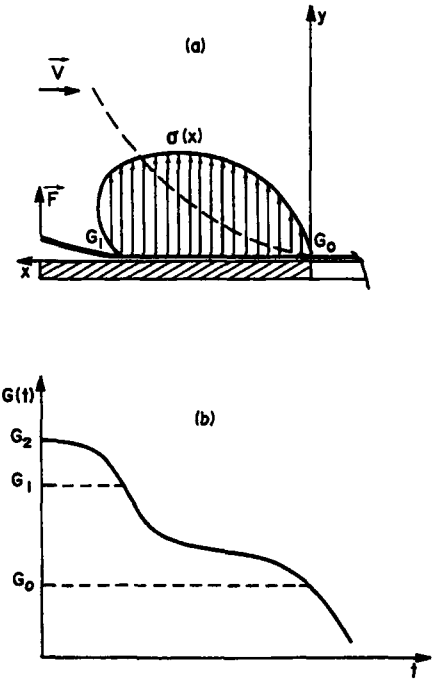

FIGURE 8 A phenomenological explanation of the stick-slip phenomenon.

substrate. Hence the I_2 domain may be called the "glassy interfacial fracture domain".

3.2.1. A Phenomenological Model of Stick-slip Behavior

Maugis [12] has presented a stick-slip model which corresponds to an hysteresis cycle between two branches of the peeling force *versus* peeling rate curve. As we did not observe another "positive branch" at the highest peeling rates, we rather think that, in the stick-slip domain, the crack first accelerates and propagates at velocities much higher that the velocity imposed by the testing machine, but the crack length is limited by the viscoelastic nature of the material. High peeling rates correspond to high frequencies for the rheological data obtained in the frequency domain (mechanical spectroscopy) or to short times for the rheological data obtained in the time domain (stress relaxation, creep).

So at high peeling rates the I_2 fracture domain corresponds to a brittle fracture of the material which behaves like an organic glass. But the crack length is limited and the material surrounding the crack behaves like a rubber at moderate times of deformation or like a highly viscous liquid at large times of deformation (which is the case away from the crack tip). So the crack is damped and the machine will recover the crack length and peel the material again. This leads to the cyclic process of stick-slip which is observed all along the peeled probe (see Fig. 8).

The recorded force in the stick-slip region does not get back to zero at the minimum of the oscillations. The small residual value may be due to the compliance of the testing machine or to the stresses generated by the strong plastic deformation of the flexible substrate.

3.2.2. The Glassy Interfacial Fracture Domain

This fracture zone corresponds to the glassy plateau of the viscoelastic behavior. The variations of the glassy modulus with addition of resin were small (less than 15%), hence the glassy modulus may be considered the same for all formulations as a first approximation. The adhesive formulation behaves as a glass in that region and does not experience any observable macroscopic deformation. Fracture propagates between the glassy material and the flexible substrate which has a very small (less than 1 mm) radius of curvature in that peeling domain. The adherence properties in this region are very poor because of the brittle behavior of the material accompanied by low viscoelastic losses.

3.3. Time-temperature Equivalence

The peeling master curves obtained by applying time-temperature equivalence (Figs. 4–6) exhibit the various peeling domains. Comparing the values of the rheological shift factors with the shift factors of the peeling curves leads to the conclusion that both are identical within experimental uncertainties and do not depend on the fracture mode (Fig. 9). So one may conclude that the rheological properties govern the adherence properties when surface energy is large enough to generate a stress field within the adhesive. As already mentioned [1], this result is counterintuitive, especially in the glassy

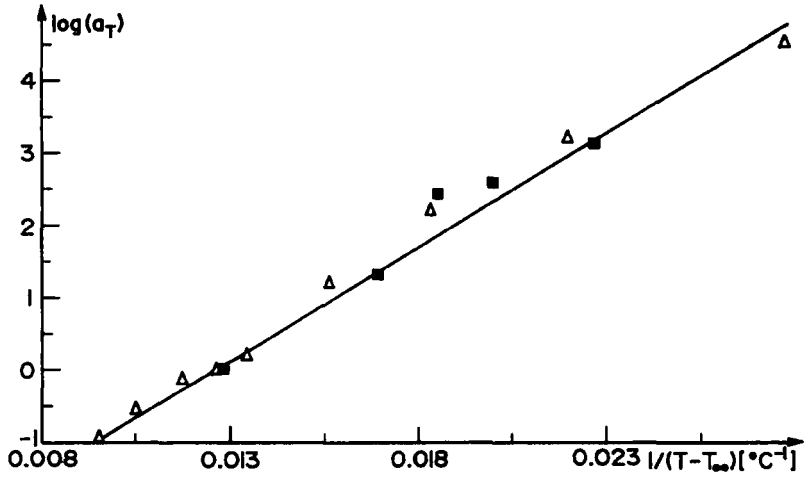

FIGURE 9 Comparison between the temperature shift factors obtained in the peeling and rheological experiments for sample 35PB165. (Δ: a_T rheology; ■: a_T peeling; reference $T_0 = 25°C$).

domain where sample deformation and viscoelastic losses are small. It is indeed the identity of the shift factors which is a proof of the adhesive deformation even in that domain. So we think that the glassy domain could also bring information on interfacial properties (*i.e.*, surface energy), such information being generally searched at vanishing peeling rates. One important question is: do we change the stick-slip peeling rate upon changing the rigid substrate nature or are the viscoelastic properties really dominant? Gent and Petrich [2] have described such an effect on the cohesive to interfacial transition, but the question remains open for the (rubbery) interfacial to stick-slip transition.

4. CALCULATION OF PEELING CURVES. COMPARISON WITH EXPERIMENTS

In Refs. [1] and [3] we proposed a description of the peeling test which allowed one to derive the peeling force, F, calculated from the test geometry and the viscoelastic properties of the adhesive. Let us recall the main elements of the previous analysis. We have defined [1]

an open system, S, as the bent part of the flexible aluminium foil. We may use the angular moment law which states that the sum of moments of forces exerted on the system may be written as:

$$\frac{d\vec{\sigma}_0}{dt} + \vec{V}(O) \wedge m\vec{V}(G) + q_m\left(\overrightarrow{OO'} \wedge \vec{V}(O') - \overrightarrow{OM} \wedge \vec{V}(M)\right) = \sum \vec{M}_{/0}(\vec{F}_{ext}) \quad (1)$$

where $\vec{\sigma}_0$ is the angular moment of the aluminium foil, $\vec{V}(O)$ is the velocity of point O, $\vec{V}(G)$ is the velocity of the center of gravity of the bent part of the aluminium foil, and q_m is the mass flow through the system S (see Fig. 10 where the system is described).

The velocity is 0 at point O. A peeling test is performed at constant peeling rate so we are in stationary conditions. The system is equivalent to a system at equilibrium, so: $d\vec{\sigma}_0/dt = \vec{0}$; furthermore,

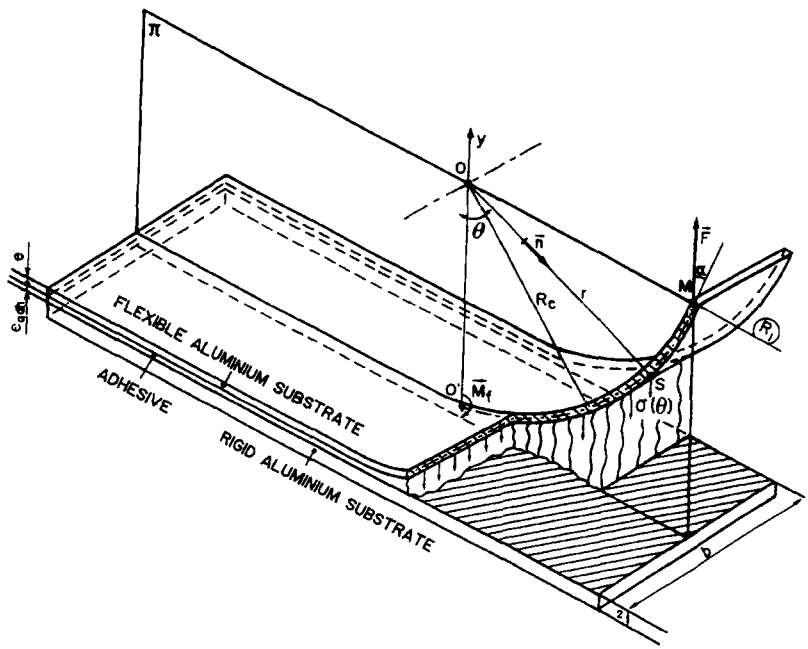

FIGURE 10 Schematic of the "System" S.

the last term of the left handside of Eq. (1) is also 0 in stationary conditions:

$$q_m\left(\overrightarrow{OO'} \wedge \vec{V}(O') - \overrightarrow{OM} \wedge \vec{V}(M)\right) = \vec{0}, \quad \text{hence we get at time } t\text{:}$$

$$\sum \vec{M}_{/0}(\vec{F}_{\text{ext}}) = \vec{0} \tag{2}$$

The various forces acting on the flexible substrate are indicated on Figure 10. Before analysing the effects of these forces in terms of their moments, we have to make some hypotheses:

- The moment created by the weight of the isolated curved part of the aluminium is negligible.
- We assume that the aluminium foil is linked to point O' which is a fixed point in a coordinate system linked to the aluminium foil.
- There is no sliding between the flexible aluminium and the mobile roller.

Remark: With respect to a Galilean laboratory coordinate system (R), the chosen coordinate system linked to the rigid aluminium substrate (R') has a uniform rectilinear translation motion and is also Galilean. One may apply then the fundamental laws of solid dynamics with respect to coordinate system R'.

Let us consider a point M belonging to the trace of the neutral fiber in plane (II), which is the vertical plane of symetry of the system. M is the application point of the force $\vec{F}$. All the forces and stresses generated are located in plane (II). In a linear (elastic) behaviour domain, the balance of moments applied to the system is:

$$\vec{M}_{/0}(\vec{F}) + \vec{M}_f + \int_0^{\theta_M} \vec{M}_{/0}(\vec{\sigma}(\theta)\, dS)\, d\theta = \vec{0} \tag{3}$$

These three moments are, respectively, the moment with respect to O of the applied force $\vec{F}$: $\vec{M}_{/0}(\vec{F})$, the bending moment of the aluminium foil $\vec{M}_f$, the moment with respect to O of the stresses generated by the adhesive and the moment with respect to O of the

shearing stresses. The detailed calculation of the three moments [1] leads to the expression of the peeling force:

$$F = \frac{b}{r_M}\left[\int_{-e/2}^{e/2} \sigma'(z) z \, dz + \int_0^{\theta_M} (\vec{\sigma}(\theta) \wedge r^2 \vec{n})\vec{k} \, d\theta + \rho e V^2\right] \quad (4)$$

where b is the sample width; r_M, e and ρ, respectively, the radius of curvature, thickness and density of the aluminium foil; σ' and σ the stresses within, respectively, the aluminium foil and the adhesive. θ_M is the maximum angle of attachment of the adhesive along the curved part of the aluminium foil. In the domain of our experimental peeling rates (V), the last term of Eq. (4) ($\rho e V^2$) is negligible [3], and this term will be neglected in the subsequent calculations.

We have simplified that equation assuming that the radius of curvature is constant and equal to the average radius of the neutral fiber, R_c [1]. Hence $r_M = R_c$ and $r = (R_c + e/2)$. We have assumed also that each volume element of the adhesive experiences an elongational deformation: hence one neglects the shear deformation and the stresses are oriented in the y-direction:

$$\vec{\sigma}(\theta) \wedge \vec{n} = \sigma(\theta) \sin\theta \, \vec{k}$$

and Eq. (4) becomes:

$$F = \frac{b}{r_M}\left[\int_{-e/2}^{e/2} \sigma'(z) z \, dz + \left(R_c + \frac{e}{2}\right)^2 \int_0^{\theta_M} \sigma(\theta) \sin\theta \, d\theta\right] \quad (5)$$

In the cohesive fracture domain [1], the maximum angle, θ_M, was defined by a fracture criterion corresponding to a maximum elongational strain of 4.5 Hencky which is independent of the peeling rate, this being consistent with uniaxial elongation measurements performed on these adhesive samples. This large value of the maximum Hencky strain (4.5) is typical of monodisperse entangled polymers. In the case of commercial adhesives formulated from polydisperse polymers, the maximum Hencky strain is smaller (≈ 3). As precised below, the real fracture criterion has been taken as 90° whenever the critical Hencky strain could not be reached (corresponding to a smaller Hencky strain). It has been found that this occurs at

the end of the cohesive fracture domain and/or at the beginning of the interfacial 1 fracture domain.

For the interfacial fracture domain, we have to define another fracture criterion which has to coexist with the first one. In order to define this fracture criterion, we have used the qualitative model of de Gennes [6] generally known as the "trumpet model" of viscoelastic fracture.

4.1. The "Trumpet Model"

This model [6] gives a new picture of the shape of the crack in a viscoelastic solid submitted to a given stress field. The model yields to a trumpet-like shape of the crack, the different parts along the crack matching the various viscoelastic domains exhibited as a function of time (or frequency). This highly qualitative picture has been formalized by Huy *et al.* [13], leading to a quantitative description of the initial concept of de Gennes. The main result is that most of the energy dissipation may extend far away from the crack tip, along a crack which may be spatially very large (Fig. 11); hence, this description is completely different from the usual picture of fracture mechanics in solids. The ratio of the elastic moduli before and after a viscoelastic transition (here from the rubbery to glassy behavior) creates an "amplifying factor" for the fracture energy which explains that the peeling energy is essentially a viscoelastic function and that its value may be several order of magnitudes larger than the Dupré surface energy. This explains qualitatively the large amplifying factor obtained with lightly-crosslinked pressure sensitive adhesives. The "trumpet" model, however, based on elaborate concepts of fracture mechanics, gives a clear picture of the main features of the fracture mechanisms of a viscoelastic material. In particular, the relation:

$$\sigma u = \text{constant}, \tag{6}$$

where σ is the stress on the crack lip and u is the crack opening, is indeed a "fracture criterion" in the domains where the material behaves like an elastic solid. This equation leads to a result which is equivalent to what is obtained from the Rice integral [14] where the fracture energy is a constant, whatever the material, for a given value of the product of σu.

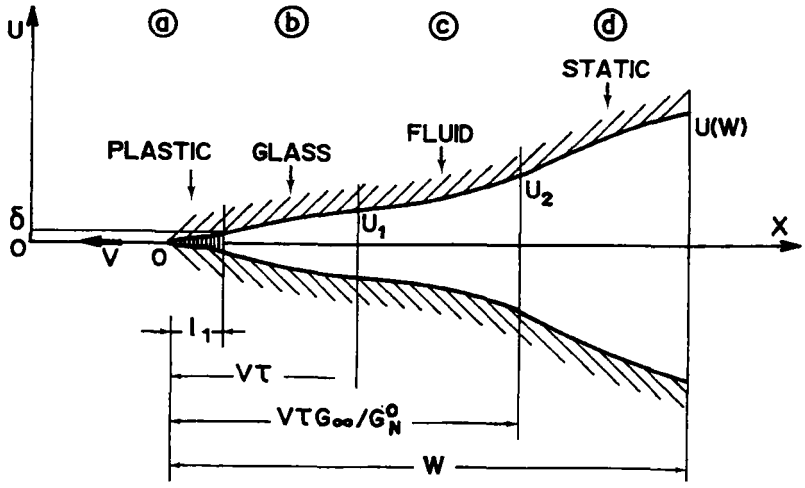

FIGURE 11 A schematic view of the "trumpet" following the picture of de Gennes. w is the adhesive thickness.

4.2. Calculation of the Peeling Behavior in the Interfacial Fracture Domain

As in the first paper of this series, the peeling force has been calculated from Eq. (5). We need in this equation (i) a constitutive equation for the viscoelastic behavior of the material to calculate the transient stress, $\sigma(\theta)$, and (ii) a fracture criterion defining the maximum integration angle, θ_M.

4.2.1. Constitutive Equation

We have used a non-linear integral constitutive equation of the KBKZ [1, 15, 16] type which describes fairly well the viscoelastic behavior of polymers in strong flows:

$$\sigma(t) = \int_{-\infty}^{t} m(t - t')h(\lambda)\tilde{C}_t^{-1}dt' \tag{7}$$

where $m(t)$ is the memory function derived from linear viscoelastic measurements, $h(\lambda)$ is a damping function depending on the strain, λ,

and $\tilde{C}_t^{-1}$ is the Finger strain tensor. The memory function is related to the relaxation modulus by:

$$m(t) = -\frac{dG(t)}{dt} \tag{8}$$

The relaxation modulus, $G(t)$, may be derived from the complex shear modulus, $G^*(\omega)$, by an inverse Fourier transform. In our case, all these functions, derived from molecular models, are analytical [7]. For uniaxial deformation, the Finger deformation tensor is given by:

$$\tilde{C}_t^{-1} = \lambda^2 - \frac{1}{\lambda} \tag{9}$$

where λ is the local strain of the material during a peeling test.

Equation (7) contains an *ad hoc* function (the damping function, h) which corrects for the too-large strains predicted by the Lodge "elastic liquid" [17] constitutive equation ($h(\lambda) = 1$). The damping function we have used in our calculations has been given by Wagner [16] and fits the non linear data in shear and elongation for a large number of linear polymers.

$$h(\lambda) = [\lambda^2 \exp(-m) + \lambda^a(1 - \exp(-m))]^{-1} \tag{10}$$

with $m = 4$ and $a = 0.3$.

4.2.2. Fracture Criterion

We have at first attempted to use Eq. (6): $\sigma(\theta_M)\, u(\theta_M) = cte$, as a fracture criterion in the interfacial 2 fracture domain, where the behavior is mainly elastic (glassy). The crack opening, u, is defined as (see Fig. 12):

$$u(\theta_M) = e_{adh}\, \varepsilon(\theta_M) \tag{11}$$

e_{adh} being the adhesive thickness and $\varepsilon(\theta_M)$ the maximum strain value, corresponding to θ_M. So, in the glassy region, assuming a perfectly elastic behavior and using de Gennes fracture criterion, we have postulated that:

$$\sigma(\theta_M) u(\theta_M) = e_{adh}\, G_\infty \tag{12}$$

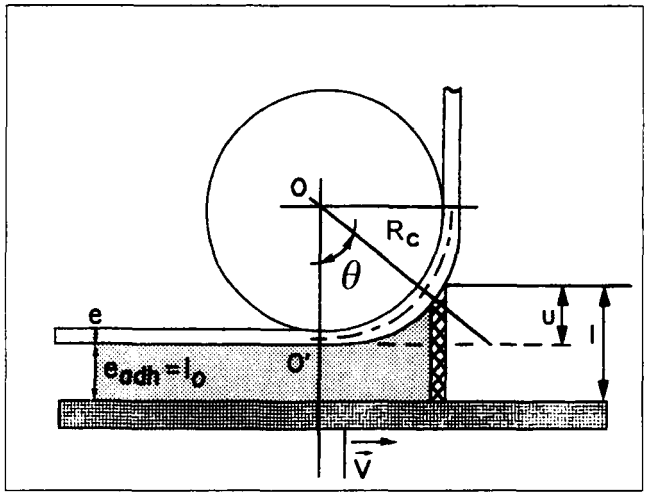

FIGURE 12 A schematic of the adhesive deformation during a peeling test.

which leads to peeling forces close to the experimental values in the interfacial 2 (glassy) fracture domain. In that case, the product σu is the only fitting parameter of the model. To perform the calculation of the peeling force F, Eq. (4), we have to determine the maximum angle, θ_M, corresponding to the upper limit of integration of σ. θ_M has been determined by an iteration procedure to match the selected fracture criterion Eq. (2), using Wagner's constitutive equation for σ. In some cases (beginning of the interfacial 1 domain), the fracture criterion could not be matched for θ_M values smaller than 90°, so the integration has been performed up to a fracture angle corresponding to $\theta_M = 90°$.

In order to minimize the number of physical parameters (or avoid additional adjustable parameters), we have used the same fracture criterion (Eq. 12) in the whole interfacial fracture domain (I_1 and I_2). We are aware that this procedure is highly questionable, particularly in the stick-slip domain, where the behavior is highly viscoelastic (see discussion below). This approach will need further investigation; one possibility would be also to use the plateau modulus instead of the glassy modulus in the fracture domain I_1 corresponding to the rubbery (highly elastic) behavior of the adhesive. In the present context we have kept the same fracture criterion in the whole interfacial fracture

domain, which leads to a very good fit for all formulations, without any adjustable parameters. The solid lines of Figures 4 and 5 correspond to peeling curves calculated using the mechanical model described in Refs. [1] and [3] along with the above fracture criterion. The experimental peeling force levels are well predicted in each domain *as well as the location of the cohesive to* I_1 transition; the two criteria coexist in the model, the transition from one criterion to the other (deformation criterion in the cohesive domain to an energy criterion in the I_1 domain) arising upon reaching the critical value of σu defined in Eq. (12). The other transition (I_1 to I_2) is a purely rheological transition due to the strong increase of the moduli when one shifts from the rubbery to glassy behavior. A critical test of the validity of the fracture criterion selected here (Eq. (12)) would be to check the effect of the adhesive thickness on the peeling force values as well as the location of the transitions. A critical evaluation of the fracture criteria on a wide variety of adhesives as a function of adhesive thickness is one of the developments of the present work. We have already performed some calculations in the cohesive to I_1 fracture domain at different sample thicknesses (Fig. 13) and it appears that this transition is shifted to higher peeling rates as the adhesive thickness increases, in agreement with the literature data [18].

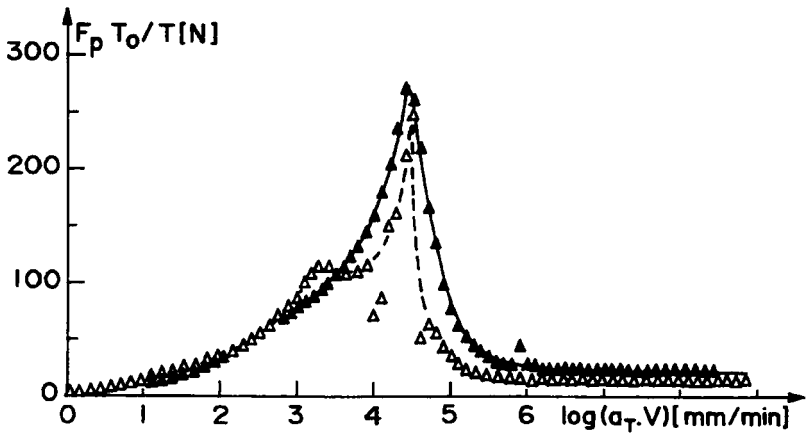

FIGURE 13 The effect of sample thickness on peeling properties (simulation from the model). ▲ $e_1 = 200\,\mu m$; △ $e_2 = 130\,\mu m$.

5. DISCUSSION: SOME COMMENTS ON FRACTURE CRITERIA

The agreement between our calculations and the experimental peeling data seems reasonable in a very wide range of peeling rates, where the rheological behavior of the adhesive is the dominant feature. This calculation includes two fracture criteria related to both fracture modes (cohesive/interfacial); these criteria are, however, independent of temperature, peeling rate and even adhesive formulation for an homologous series of samples. These two criteria coexist and predict with a reasonable approximation the cohesive to I_1 transition. At every peeling rate value, the computer program calculates the adhesive deformation and the (σu) product. If the sample reaches the critical strain before reaching the critical value of σu, the strain criterion is selected (cohesive fracture domain); otherwise, the energy criterion which corresponds to higher peeling rates is selected. The shift from one criterion to the other defines the cohesive to I_1 transition. One may easily understand the fracture criterion corresponding to a critical strain in the cohesive domain, in which the deformation of the adhesive is essentially a flow process, but the fracture criterion selected in the I_1 and I_2 domains is certainly oversimplistic. It seems difficult to understand why the same criterion would apply in the rubbery and glassy domains (*i.e.*, I_1 and I_2 fracture domains), with no effect of the interface. So an interface-dependent constant appearing in the relation ($\sigma u = ct$) could also be estimated numerically in the I_1 and I_2 domains from the peeling data. We are working now on a critical study of fracture criteria in the interfacial fracture domain, changing the substrate nature, adhesive nature and thickness; the present approach has the merit to describe, qualitatively and quantitatively as a first approximation, the main features of the fracture process of a highly viscoelastic adhesive, with no adjustable function or parameter. Besides, the conjunction of the two criteria defined above seems to explain also the effect of sample thickness on the adherence properties and fracture mode transitions: we have plotted on Figure 14 the data of Aubrey [18] related to the effect of the adhesive sample thickness with the cohesive to interfacial transition, compared with our model (see Fig. 13 and related comments). "Thickness ratio" means the ratio of thicknesses (for the same material) which is plotted as a function of

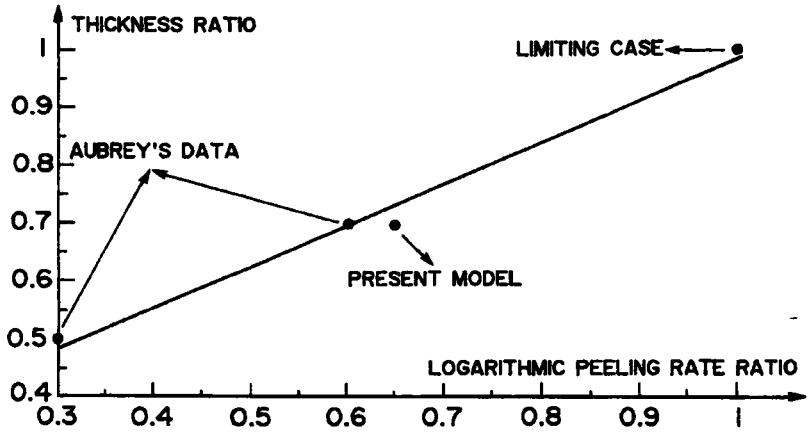

FIGURE 14 The model gives a reasonable qualitative picture of the effect of sample thickness: comparison with the data from Aubrey [18].

the ratio of the respective peeling rates corresponding to the cohesive-interfacial transition, in a semi-logarithmic scale.

6. CONCLUSION: THE INTEREST OF STUDYING MODEL FORMULATION

The study of structurally well-defined adhesives has proved and quantified the link between rheology and adherence. We have been able to provide an original approach in linking the peeling parameters to rheological parameters. It is clear, however, that the analysis performed in the interfacial domain is not as elaborate as what had been done in the cohesive domain [1]. It confirms, however, the essential role played by the rheological properties in the whole range of peeling rates and provides a significant advancement for future studies.

The formulations made from monodisperse samples exhibit well-defined rheological and peeling transitions, allowing a quantitative study of their relationship. Besides, the use of models of molecular dynamics allow one to calculate the viscoelastic properties of the formulations, yielding an elaborate and quantitatively-predictive tool of adhesive formulation. We have shown that cohesive fracture was governed by the slowest relaxation processes: the reduced peeling

curve, $F(V\tau_0)$, where τ_0 is the relaxation time of the terminal region of mechanical relaxation, is a master curve for all formulations. In the same way, each peeling domain matches a viscoelastic behavior domain. This model, presented here in the case of model formulations, has been applied successfully to a large number of commercial adhesive formulations. If these data may not be published, for obvious reasons, one may say that the link between viscoelastic relaxation domains and fracture domains has been clearly confirmed: with an adequate heat treatment, it is possible to make the flow region (hence cohesive fracture) disappear for some formulations. In the same way, the interfacial 1 fracture disappears when the plateau region is suppressed by adequate formulation.

Acknowledgements

C. D., A. A. and G. M. thank the ElfAtochem Company (Groupement de Recherches de Lacq) for financial support of this work. The Michelin Company is also gratefully acknowledged for the synthesis of the monodisperse polybutadiene samples.

References

[1] Derail, C., Allal, A., Marin, G. and Tordjeman, Ph., *J. Adhesion* **61**, 123 (1997).
[2] Gent, A. N. and Petrich, R. P., *Proc. Roy. Soc. London* **A300**, 433 (1969).
[3] Derail, C., Ph. D. Thesis, Université de Pau (1995).
[4] Derail, C., Benallal, A., Marin, G., Tordjeman, Ph. and Bourrel, M., *Le Vide* n°277, 168 (JADH95) (1995).
[5] Ferry, J. D., *Viscoelastic Properties of Polymers* 3rd edition (J. Wiley, N.Y., 1970).
[6] de Gennes, P. G., *C. R. Acad. Sci.* **307 II**, 1949 (1988).
[7] Benallal, A., Marin, G., Montfort, J. P. and Derail, C., *Macromolecules* **26**, 7229 (1993).
[8] Marin, G., Vandermaesen, Ph. and Komornicki, J., *J. Adhesion* **35**, 23 (1991).
[9] Aubrey, D. W. and Scheriff, M., *J. Polym. Sci.* **18**, 2597 (1980).
[10] Colby, R. H., Fetters, L. J. and Graessley, W. W., *Macromolecules* **20**, 2226 (1987).
[11] Maugis, D., *J. de Chimie-Physique* **84**(2), 217 (1986).
[12] Maugis, D., *J. Adh. Sci. Technol.* **1**(2), 105 (1987).
[13] Hui, C. Y., Xu, D. B. and Kramer, E. J., *J. Appl. Phys.* **72**(8), 3294 (1992).
[14] Rice, J. R., *J. Appl. Mech. Trans. ASME* **90**, 379 (1968).
[15] Bernstein, B., Kearsley, E. A. and Zapas, L. J., *J. Appl. Polym. Sci.* **21**, 2817 (1977).
[16] Wagner, M. H., *Rheol. Acta* **18**, 681 (1979).
[17] Lodge, A. S., *Elastic liquids* (Academic Press, New York, 1964).
[18] Aubrey, D. W., Welding, G. N. and Wong, T., *J. Appl. Polym. Sci.* **13**, 2193 (1969).

APPENDIX

Calculation of the molecular weight between entanglements for sample 30PB270: The experimental data of the variations of the plateau modulus, G_N^0, of concentrated solutions of polymers gives a power law exponent lying between 2 and 2.3, in agreement with the existing models of molecular dynamics (reptation). The observed exponent in our case was 2.27 [1], so:

$$G_N^0 = \frac{\phi RT}{M_e} \propto \phi^{2.27} \Rightarrow (M_e)_{\text{solution}} = (M_e)_{\text{bulk polymer}}\, \phi^{-1.27}$$

ϕ being the polymer volume fraction, T the temperature and M_e the molecular weight between entanglements. The molecular weight between entanglements, M_e, of bulk polybutadiene being 1900, the value of M_e for the formulation containing 30% polymer may be estimated to be close to 8800 g/mol, the molecular weight of sample PB2 being 65000 g/mol; hence, the 30PB270 formulation is still entangled.